

# Research and Design of a Polarization Multiplexed 1-Bit Reconfigurable Metasurface for Dynamic Focusing

Bo Yin<sup>1</sup>, Zhu Xu<sup>1, \*</sup>, Shubin Wang<sup>1</sup>, and Maohai Ran<sup>2</sup>

**Abstract**—To solve the problems of traditional reflective metasurfaces that cannot change the focal position and have simple functions, a polarization multiplexed 1-bit reconfigurable metasurface is proposed. It can realize the independent focusing characteristics of  $x$ -direction polarization and  $y$ -direction polarization incident waves. The metasurface unit consists of a layer of dielectric substrate with a thickness of  $0.055\lambda$ , a metal element embedded with a pair of PIN diodes, and ground. Two diagonal slits on the ground can not only be used as a reflection ground to keep high reflection, but also behave as a bias control line to control the voltage to change the state of the PIN diodes. Optimizing the structure parameters of the metasurface unit, the reflection phase can be manipulated binarily between  $0$  and  $180^\circ$ , corresponding to ON and OFF states, respectively. Based on the principle of quasi-optical path, a polarization multiplexed 1-bit reconfigurable metasurface with independent dynamic focusing characteristics at 11 GHz is designed. On this basis, by changing the polarization direction of the incident wave, the dual-focus distribution with different power ratios can be obtained. The proposed 1-bit reconfigurable metasurface has no multilayer metal elements and complex feeding structures, and has the characteristics of a simple structure, low profile, and multifunction. At the same time, it enhances the utilization of metasurface array and provides a higher degree of freedom for wireless power transmission applications in future.

## 1. INTRODUCTION

Metasurfaces, as two-dimensional metamaterials, can flexibly control electromagnetic wave properties, such as amplitude, phase, and polarization, so attracted more and more attention from scholars [1, 2]. Based on the theory of electromagnetic wave regulation, metasurfaces are widely used in many aspects such as antennas [3], polarization converters [4], perfect absorbers [5], invisibility cloaks [6], and near-field focusing [7]. However, most of studies on antennas focus on their far-field radiation characteristics. According to the theoretical study of antenna aperture field, the electric field strength of narrow beam in far-field region can be calculated, and the magnitude of the maximum electric field strength is not greater than  $2E$ , where  $E$  is the initial electric field of the transmitting antenna [8]. It can be seen that there is a clear upper limit to the convergence of high-gain beam on electromagnetic wave energy in far-field region. According to the traditional antenna theory, the power of receiving antenna can be enhanced by increasing aperture of transmitting antenna. However, considering the processing cost of practical engineering, it is unrealistic to continuously increase the aperture of transmitting antenna. Therefore, the near-field electromagnetic properties of antennas have attracted attention [9]. In the near-field region, there are certain phase differences of the electromagnetic waves in different paths, so the propagation direction of radiation waves can be adjusted by changing phase distribution, and then

---

Received 27 February 2023, Accepted 10 April 2023, Scheduled 6 May 2023

\* Corresponding author: Zhu Xu (1826113722@qq.com).

<sup>1</sup> School of Optoelectronic Engineering, Chongqing University of Posts and Telecommunications, Chongqing 400065, China. <sup>2</sup> Chongqing Electric Power College, Chongqing 400065, China.

focusing effect can be achieved [10]. Near-field focusing is a unique electromagnetic property in the near-field region. In [11], Zhang et al. designed a cross dipole element and formed an array. The array uses a horn as a feed source to focus in the near-field area and uses the polarization independence of the element to generate the focus at different positions. At the same time, by changing the orientation of the horn antenna, the distribution of the feed and focus will also change synchronously, which greatly improves the practicability of the same metasurface array. In [12], Wang et al. proposed an octagonal metasurface unit embedded circular patch operating at 10 GHz. Using the plane near-field scanning system, the single metasurface array with  $27 \times 27$  units has been designed, manufactured, and measured in the X band. The measured results are in good agreement with the simulation ones of the proposed metasurface. Zhang et al. proposed a metasurface unit with high efficiency, and it integrates reflection and transmission array functions in [13]. The proposed unit is composed of two layers of dielectric substrate and three layers of metal layer. It can focus on the near-field with different  $x$ -direction polarization and  $y$ -direction polarization. The final measured results are in good agreement with the simulation ones. Shang et al. designed a metasurface using double layers cross-dipoles reflection units to achieve independent focusing effect under different polarizations in [14]. However, the above metasurfaces are passive. They have fixed structures and no reconfigurable factors. Therefore, the functions are statically executed [15]. At the same time, in order to achieve dual-polarization independent focusing characteristics, most of them adopt the form of a multi-layer structure to achieve  $360^\circ$  phase coverage. In order to dynamically adjust the electromagnetic response of metasurface, scholars have proposed reconfigurable metasurfaces. Currently, reconfigurable metasurfaces can be achieved by integrating active tunable devices, such as varactor diodes and PIN diodes in metasurface unit and modifying ground plane [16–20]. Reconfigurable metasurface can change the reflection phase distribution of focused metasurface array to achieve dynamical focusing. In [21], Ratni et al. designed a reconfigurable one-dimensional metasurface by adding a varactor diode to the unit and realized focusing in the near-field under the feed of plane wave incidence. In [22], Yu and Lin proposed a 2-bit reconfigurable metasurface unit working in the C band. Loading the PIN diodes can change the reflection phase of the unit for dynamic focusing in the near-field region. The simulation results show that the focusing efficiency of the metasurface can reach 30% at a distance of  $30\lambda$ . Han et al. proposed a 2-bit programmable metasurface unit for indoor adaptive intelligent wireless power transmission system in [17]. Using a planar near-field scanning system, a 2-bit metasurface array working at 5.8 GHz was designed, manufactured, and measured, which can dynamically focus at different near-field positions. The above reconfigurable metasurfaces can achieve dynamic focusing in the near-field region, but most of them have the problem of single function, which limits the development of reconfigurable focused metasurfaces in wireless power transmission.

A 1-bit reconfigurable metasurface for dual-polarization near-field focusing is proposed. The designed reflective metasurface has the characteristics of independent polarization controlling, which can realize the independent focus of  $x$ -direction and  $y$ -direction polarized incident waves. Adjusting the polarization direction of incident wave and the energy proportion of the  $x$ -direction and  $y$ -direction polarizations, the focus position and distribution of dual focuses can be changed accordingly. Finally, adjusting the bias voltage to control the state of the PIN diodes can maintain the dual-polarization focusing and achieve the dynamic focusing effect. The simulated results also verify the effectiveness of the design.

## 2. DESIGN OF METASURFACE UNIT

The structure of the designed metasurface unit is shown in Fig. 1. The metasurface unit is a single layer structure composed of two PIN diodes, a dielectric substrate, 4 metallic vias, and ground metallic feedlines. The dielectric substrate is made of F4B ( $\epsilon_r = 4.4$ ,  $\tan \delta = 2.5 \times 10^{-3}$ ), with a thickness of 1.5 mm. The PIN diodes are loaded in the middle of the metal patch, and the metallic vias connect the metal patch and ground, which enables the two states of the metasurface unit.

The commonly used microwave PIN diodes are mainly produced by Macom and Skyworks. The products of Macom have higher power and higher working frequency than Skyworks. The designed metasurface unit works in the Ku band, so MADP000907-14020W of Macom is selected. The equivalent series circuit of PIN diode in ON and OFF states is shown in Fig. 2, where  $R$ ,  $L$ , and  $C$  are the equivalent series resistance, inductance, and capacitance of the PIN diode, respectively. When the state of PIN

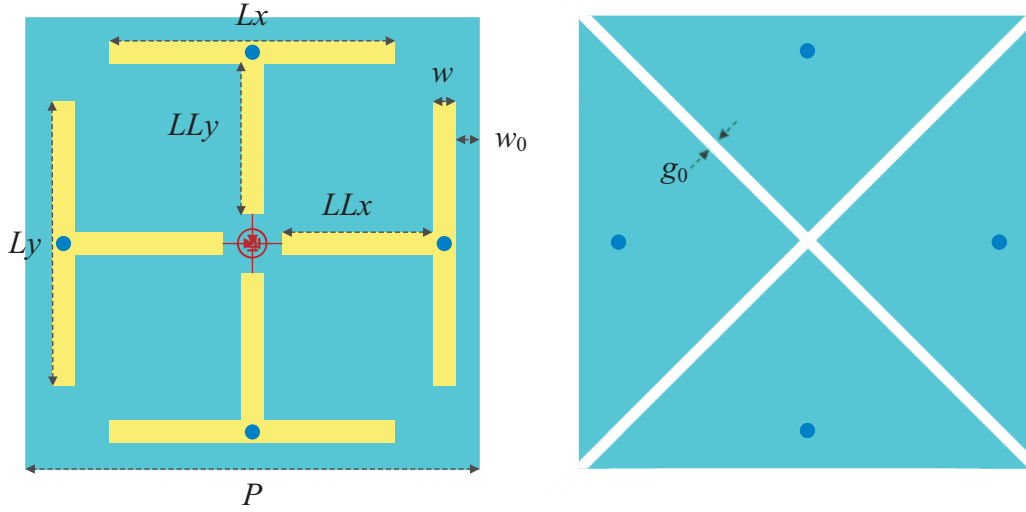


**Figure 1.** The schematic of the proposed metasurface unit structure.

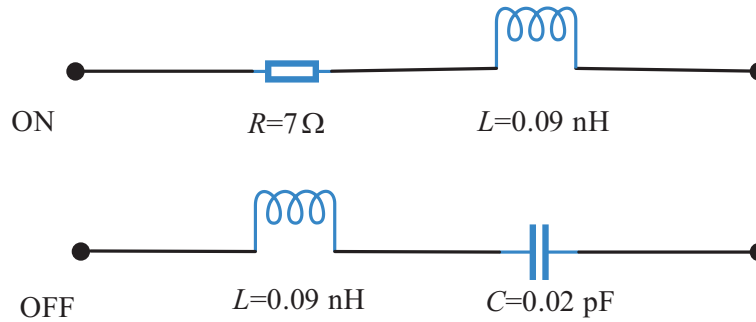


**Figure 2.** The ON and OFF equivalent serial circuits of the PIN diode.

diode is OFF,  $R = 0$ ,  $L = 0.09 \text{ nH}$ ,  $C = 0.02 \text{ pF}$ . And when the state is ON,  $R = 7 \Omega$ ,  $L = 0.09 \text{ nH}$ ,  $C = 0$ . Under the incidence of electromagnetic wave, the impedance of PIN diode can be described as:

$$\Delta\varphi(x_i, y_i) = \begin{cases} R + j\omega L & \text{ON} \\ j\omega L + \frac{1}{j\omega C} & \text{OFF} \end{cases} \cdot$$

Using CST Microwave Studio software to simulate the designed metasurface unit, the influence of ground plane loading slots on reflection coefficient is shown in Fig. 3. As shown in Fig. 3, when the state of PIN diode is ON or OFF, ground plane loading diagonal slots has little effect on the reflection amplitude at 11 GHz. This indicates that ground plane loading two diagonal slots can not only be used as a reflection ground to keep high reflection, but also behave as a bias control line to control the voltage to change the state of the PIN diodes.

When the incident wave is  $x$ -direction polarization wave, it can be seen from Figs. 4(a) and (b) that the reflection amplitude of the metasurface unit in the ON and OFF states is greater than 0.95 at 11 GHz, and the reflection phase is  $97.5^\circ$  and  $-91^\circ$ , respectively, which approximately meets the phase difference of  $180^\circ$ . Similarly, when the incident wave is  $y$ -direction polarization wave, it can be seen from Figs. 4(c) and (d) that the reflection amplitude of the metasurface unit in the ON and OFF states is greater than 0.95 at 11 GHz, and the reflection phase is  $97.5^\circ$  and  $-90^\circ$ , respectively, which approximately meets the phase difference of  $180^\circ$  and basically meets the design requirements of the 1-bit metasurface unit. In a word, whether the incident wave is a polarized wave in the  $x$ -direction or

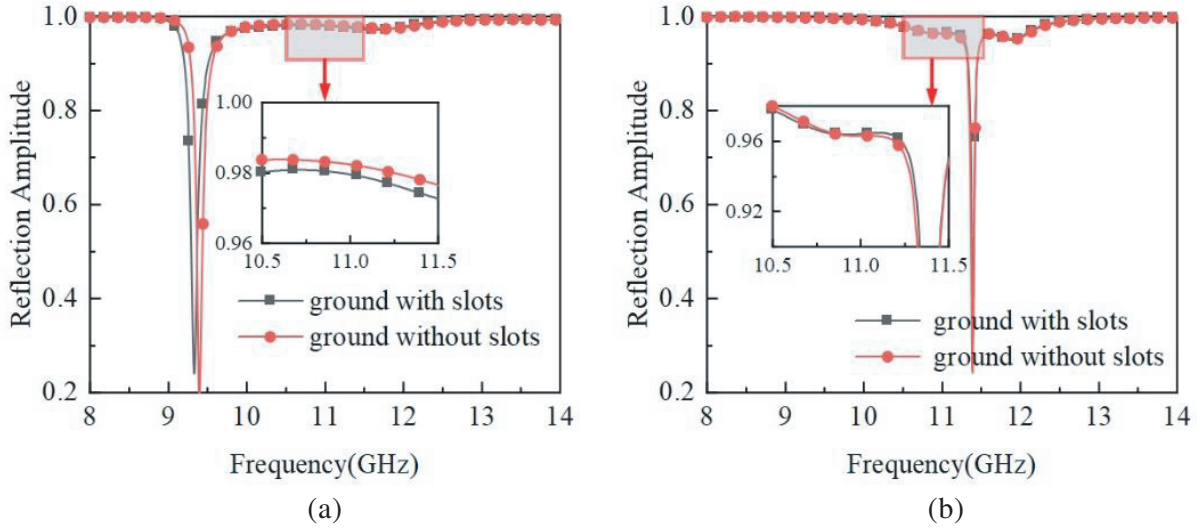


**Figure 3.** The effect of ground plane loading slots on reflection coefficient. (a) ON state. (b) OFF state.

$y$ -direction, the designed metasurface unit meets the designing requirements of a 1-bit reconfigurable focusing metasurface unit.

Another important feature to be considered is the ability of the unit to independently control dual-polarization. In order to analyze this feature, different polarization incident waves should be analyzed. When the polarization of the incident wave is in the  $y$ -direction, the state of the PIN diode in the  $x$ -direction is ON, and then the state of the PIN diode in the  $y$ -direction is changed to obtain two phase curves, as shown in Fig. 5(a). It can be seen that when the PIN diode state in the  $x$ -direction changes, the reflection phase in the  $y$ -direction has almost no change. Similarly, when the polarization of the incident wave is in the  $x$ -direction, the state of the PIN diode in the  $y$ -direction is OFF, and then changing the state of the PIN diode in the  $x$ -direction can obtain two phase curves, as shown in Fig. 5(b). From the results in the figure, when the state of the PIN diode in the  $x$ -direction changes, the reflected phase in the  $y$ -direction is almost unchanged, which shows that the state of the PIN diode in the  $x$ -direction has little influence on the reflection characteristics of the  $y$ -polarization. Similarly, from Figs. 5(c) and (d), it can be seen that the PIN diode state in the  $y$ -direction has little influence on the reflection characteristics of  $x$ -polarization. To sum up, the reflection phases in the  $x$ -direction and  $y$ -direction polarizations have little influence on each other, which well verifies the dual-polarization independent regulation characteristics of the single layer 1-bit reconfigurable metasurface unit, also an important feature in the design of polarization multiplexed metasurface. Different focusing effects can be set according to different polarizations of the incident wave, further improving the freedom of the reconfigurable metasurface in wireless power transmission.

It can be seen from Figs. 6(a) and (b) that when the incident wave is a polarized wave in the  $x$ -direction, the surface current direction on the metal patch connected by the two arms of the PIN diode in the ON state is to the right. The surface current direction on the metal patch connected to the two arms of the PIN diode in the OFF state is left. It can be seen that the surface current of the metasurface unit in the two states meets the phase difference of  $180^\circ$ , which is consistent with the phase difference of the reflection phase in Fig. 4(b). It can also be seen from Figs. 6(c) and (d) that when the incident wave is a polarized wave in the  $y$ -direction, the surface current direction on the metal patch connected by the two arms of the PIN diode in the ON state is upward. And the surface current direction on the metal patch connected to the two arms of the PIN diode in the OFF state is downward. Therefore, the surface current direction of the metasurface unit in the two states meets the phase difference of  $180^\circ$ , which is consistent with the phase difference of the reflection coefficient in Fig. 4(d). To sum up, under the excitation of polarized waves in the  $x$  and  $y$  directions, the metasurface unit meets the designing requirements of 1-bit reconfigurable metasurface unit. Therefore, the ON and OFF states can

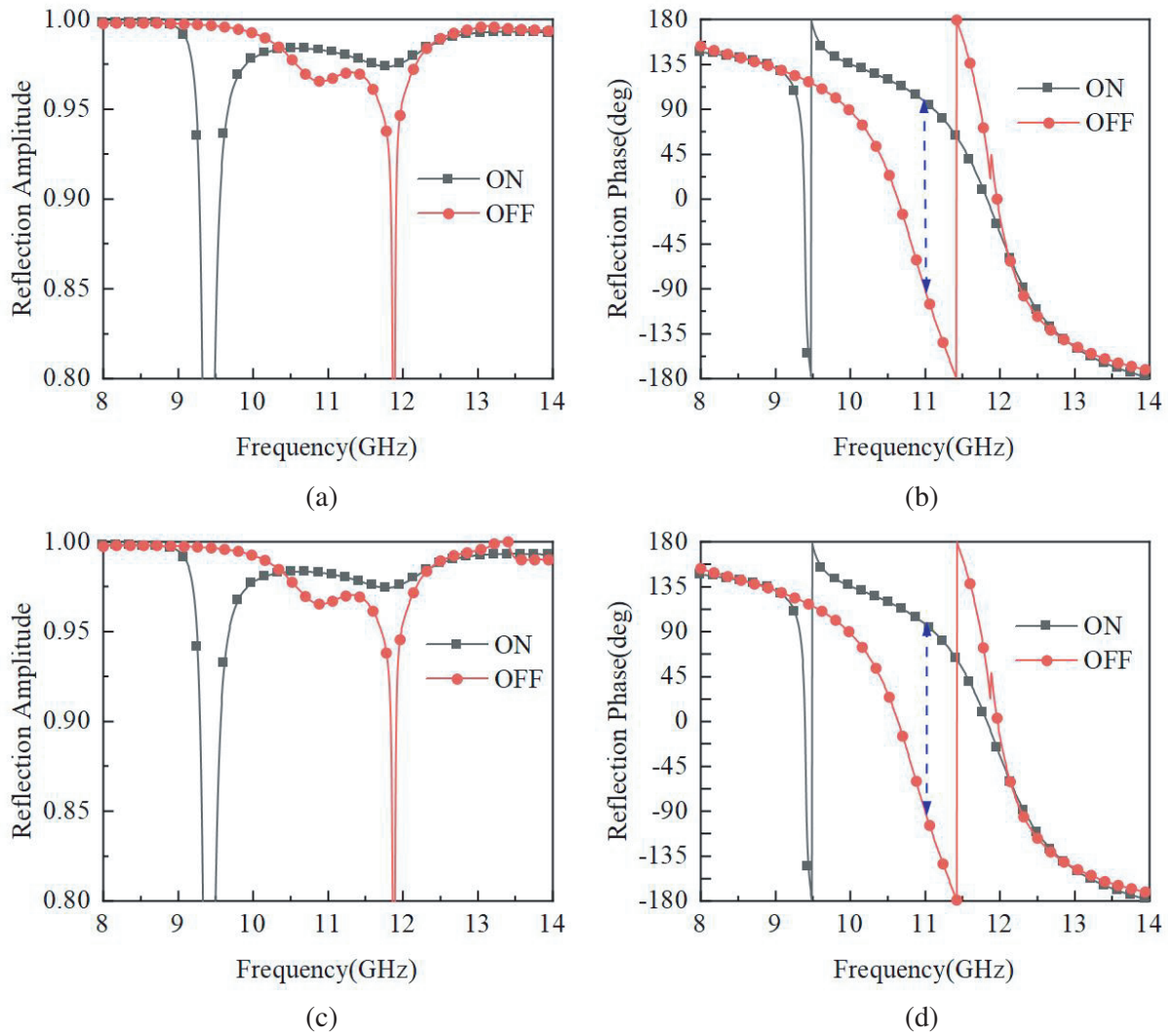


**Figure 4.** Reflection amplitude and phase curves of metasurface unit. (a) Reflection Amplitude curve with  $x$ -direction polarization excitation. (b) Reflection Phase curve with  $x$ -direction polarization excitation. (c) Reflection Amplitude curve with  $y$ -direction polarization excitation. (d) Reflection Phase curve with  $y$ -direction polarization excitation.

be corresponding to 0 and 1 in 1-bit, respectively. Other structural parameters after optimization are:  $P = 10$  mm,  $Lx = 6$  mm,  $Ly = 6$  mm,  $LLx = 3.5$  mm,  $LLy = 3.5$  mm,  $w = 0.5$  mm,  $w_0 = 0.5$  mm.

### 3. DESIGN OF METASURFACE ARRAY

#### 3.1. Near-Field Focused Metasurface Design

The schematic diagram of the designed reflective metasurface model is shown in Fig. 7. The design of reflective metasurface needs to determine the phase distribution of the metasurface according to the working frequency band of the incident wave, excitation mode, focus position, and other indicators. In order to achieve arbitrary focus trajectory, the reflection phase distributions corresponding to different focuses must be designed to convert the incident electromagnetic wave into the required focused beam. The phase distribution required by the focus can be calculated by formula (1), and the expression of

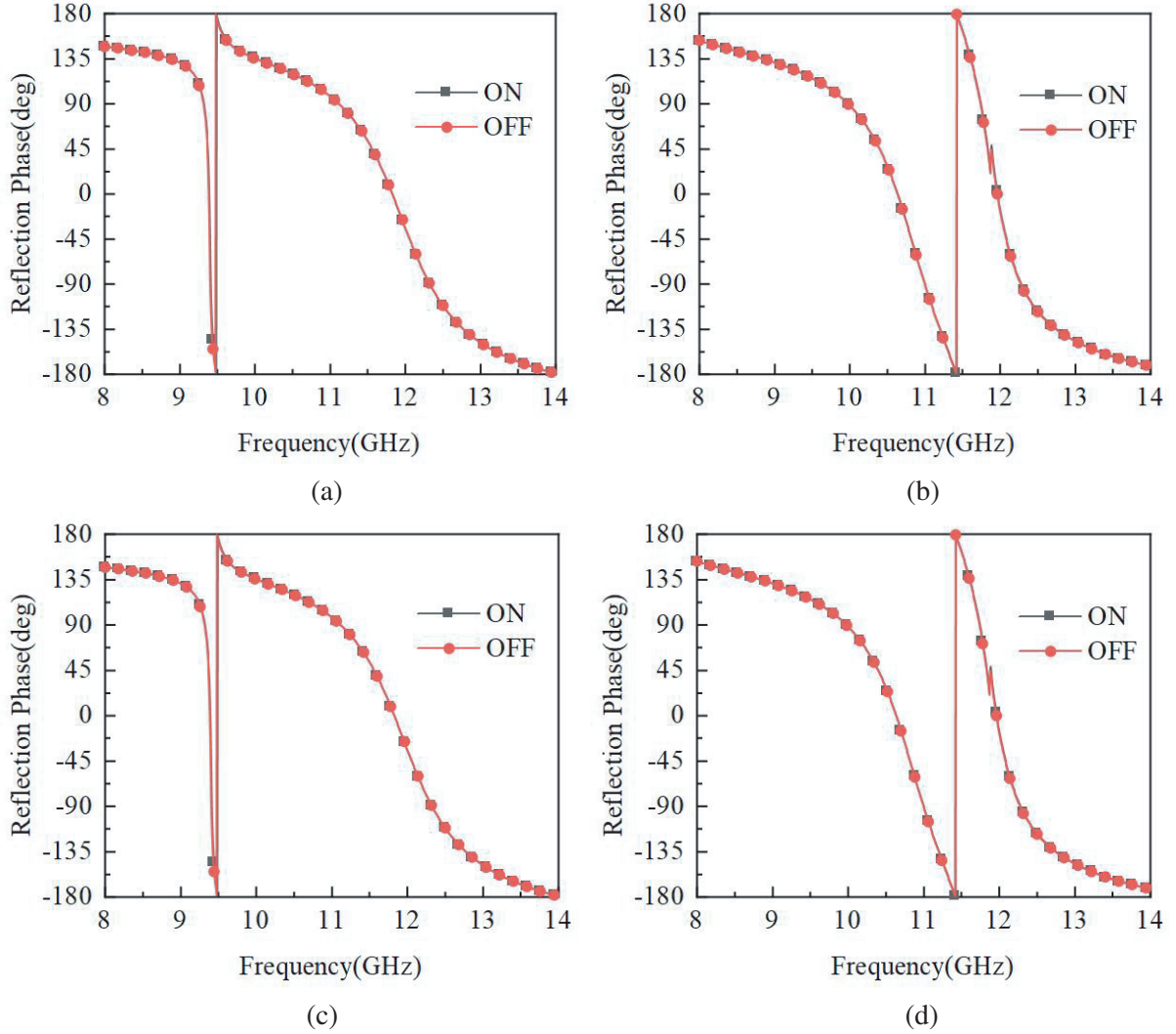


**Figure 5.** Reflection phase characteristics of polarization independent regulation. (a) Reflection Phase curve under  $y$ -direction polarization excitation with the state of PIN diode in  $x$ -direction. (b) Reflection Phase curve under  $y$ -direction polarization excitation with the state of PIN diode in  $x$ -direction. (c) Reflection Phase curve under  $x$ -direction polarization excitation with the state of PIN diode in  $y$ -direction. (d) Reflection Phase curve under  $x$ -direction polarization excitation with the state of PIN diode in  $y$ -direction.

the electric field distribution required on the reflective metasurface [23] is:

$$E(x_i, y_i) = A(x_i, y_i) \exp(j\varphi(x_i, y_i)) \quad (1)$$

where  $(x_i, y_i)$  is the center position coordinate of the  $i$ th cell;  $A(x_i, y_i)$  is the electric field amplitude corresponding to the  $i$ th cell;  $\varphi(x_i, y_i)$  indicates the electric field phase required by the  $i$ th unit.

The key of the designed reflective metasurface to control the electromagnetic wave is that the reflective units of different sizes can achieve different reflection phases.

By designing the size of each unit, adjust the reflection phase to change the propagation direction of electromagnetic wave, and achieve the purpose of metasurface focusing. According to the theory of electromagnetic wave propagation, the phase is equal to the product of wave number and wave path, and the distance between each unit on the reflecting metasurface and the target focus position is  $|\vec{r}_d - \vec{r}_i|$ . Setting the reflecting metasurface as the phase reference plane, the phase distribution required

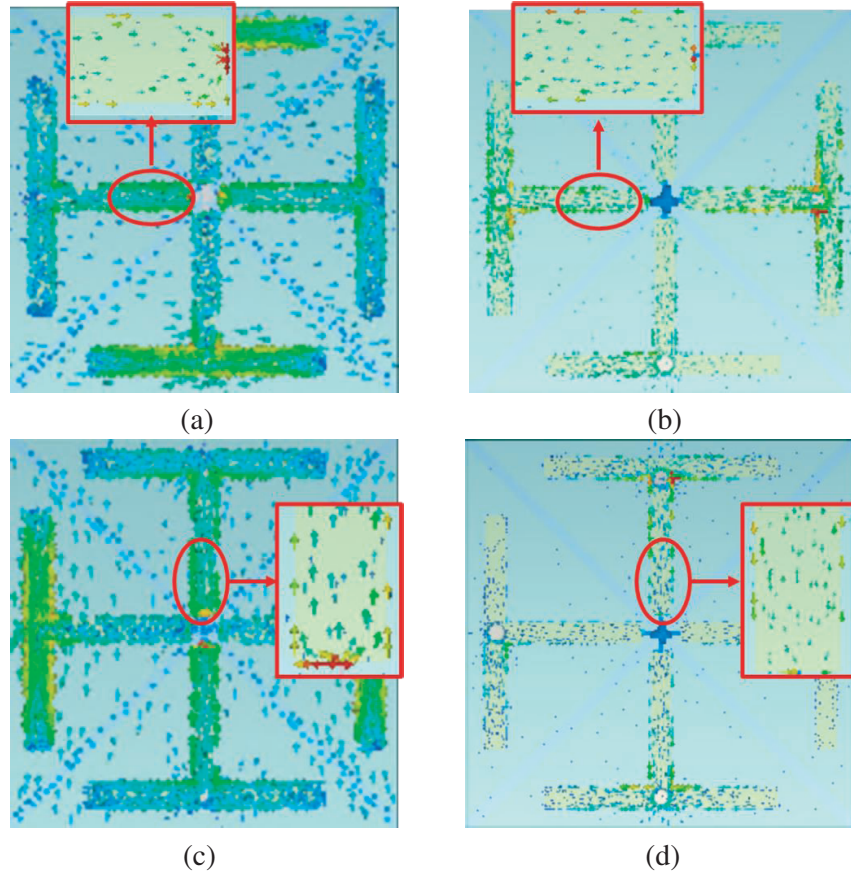


**Figure 6.** Current distribution diagram of metasurface unit. (a) Current distribution diagram with the ON state in  $x$ -direction with  $x$ -direction polarization excitation. (b) Current distribution diagram with the OFF state in  $x$ -direction with  $x$ -direction polarization excitation. (c) Current distribution diagram with the ON state in  $y$ -direction with  $y$ -direction polarization excitation. (d) Current distribution diagram with the OFF state in  $y$ -direction with  $y$ -direction polarization excitation.

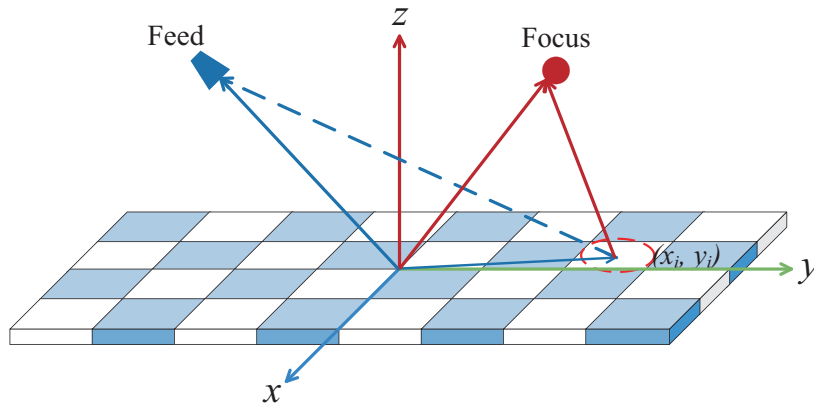


**Figure 7.** Model diagram of reflective metasurface array.

to generate the focus in space can be obtained as follows:

$$\varphi_d(x_i, y_i) = \arg(\exp(-jk_0 |\vec{r}_d - \vec{r}_i|)) = -k_0 |\vec{r}_d - \vec{r}_i| \quad (2)$$

The distance of each unit on the reflecting metasurface is  $|\vec{r}_f - \vec{r}_i|$ , and the reflecting metasurface is

still used as the phase reference plane. For the feed, the phase distribution required to generate the focus belongs to the wavefront of the reference plane, so the phase distribution required to generate the focus in space can be obtained as follows:

$$\varphi_f(x_i, y_i) = \arg(\exp(jk_0 |\vec{r}_f - \vec{r}_i|)) = k_0 |\vec{r}_f - \vec{r}_i| \quad (3)$$

The phase shift distribution required by the reflective metasurface is the difference between the phase distribution to generate the focus and the initial phase distribution caused by the feed, that is  $\varphi_f(x_i, y_i) = 0$ , so we can get:

$$\Delta\varphi(x_i, y_i) = \varphi_d(x_i, y_i) - \varphi_f(x_i, y_i) \quad (4)$$

In the formula,  $|\vec{r}_d|$  is the focus coordinate,  $|\vec{r}_i|$  the center coordinate of each element of the metasurface, and  $|\vec{r}_f|$  the feed coordinate. Since the plane wave is used as the feed source, the initial phase caused by the feed source is zero, that is,  $\varphi_f(x_i, y_i)$ . According to formula (4),

$$\Delta\varphi(x_i, y_i) = \varphi_d(x_i, y_i) = k_0 |\vec{r}_d - \vec{r}_i| \quad (5)$$

After calculating the phase information of each metasurface unit, 1-bit discrete processing is performed on the phase distribution,

$$\Delta\varphi(x_i, y_i) = \begin{cases} 0 & -90^\circ \leq \Delta\varphi(x_i, y_i) < 90^\circ \\ 180 & \text{else} \end{cases} \quad (6)$$

### 3.2. Simulation Results

According to the antenna near-field theory [20], the antenna radiation radius  $r < 2D^2/\lambda$ , where  $D$  is the maximum aperture of the antenna, and  $\lambda$  is the working wavelength of the antenna. The design objective of this paper is to achieve the focus at a distance of 250 mm from the metasurface. When the incident wave is a polarized wave in the  $x$ -direction, the focus position is (0, 150 mm, 250 mm). When the incident wave is a polarized wave in the  $y$ -direction, the focus position is (150 mm, 0, 250 mm). Based on the theoretical analysis of focusing in the previous section, the phase distribution of metasurface under different polarized incident waves is calculated, as shown in Fig. 8. The overall structure of the reconfigurable metasurface composed of  $17 \times 17$  units is shown in Fig. 9. The array size is 170 mm  $\times$  170 mm. Therefore, an electric field monitor is set at 11 GHz to view the focusing situation. The commercial software CST Microwave Studio is used to simulate the frequency point, and the electric field distribution diagram of the  $xy$  plane at the above frequency point is obtained.

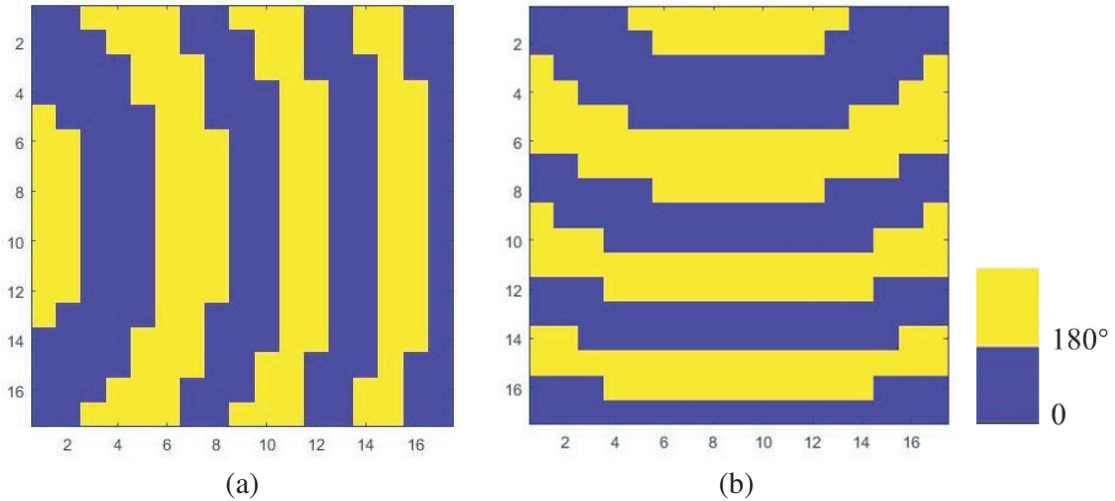


**Figure 8.** Metasurface phase distribution. (a) Metasurface phase distribution under  $x$ -direction excitation. (b) Metasurface phase distribution under  $y$ -direction excitation.

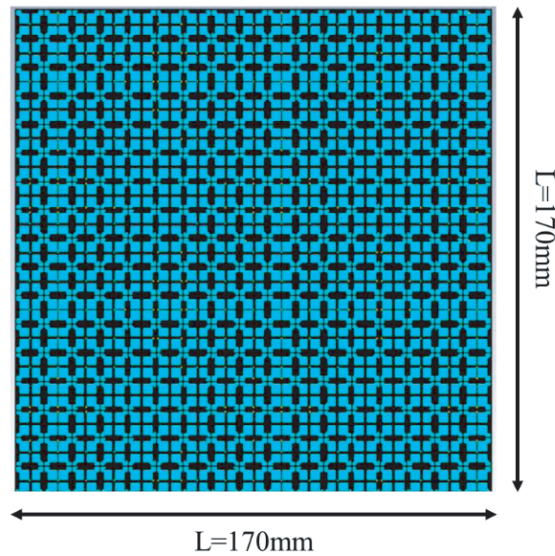


**Figure 9.** Overall structure diagram of metasurface array.

When the incident wave is a polarized wave in the  $x$ -direction, the position of target focus is  $(0, 150 \text{ mm}, 250 \text{ mm})$ . As shown in Fig. 10(a), the position of the maximum electric field intensity is  $(0, 140.1 \text{ mm}, 250 \text{ mm})$ , which is basically consistent with the target focus. Focusing efficiency is defined as the ratio of the focal energy with a focused metasurface to the plane energy at the same position without a focused metasurface array. Therefore, the focus efficiency at 11 GHz is calculated as 48% based on the Poynting theory. Finally, adjusting the ON/OFF states of the PIN diodes in the  $x$ -direction on the metasurface, the phase distribution of the metasurface array can be changed. The simulated electric field distribution of  $xoy$  plane is shown in Fig. 10(b). The target focus position is  $(0, -150 \text{ mm}, 250 \text{ mm})$ , and the position of the maximum electric field intensity in Fig. 10(b) is  $(0, -140.5 \text{ mm}, 250 \text{ mm})$ , which is basically consistent with the target focus.

When the incident wave is a polarized wave in the  $y$ -direction, the position of target focus is  $(0,$

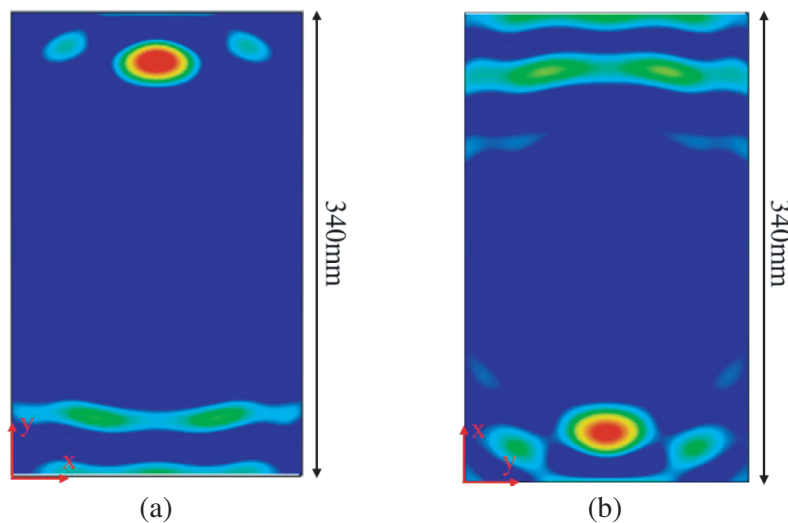


**Figure 10.** Electric field distribution of  $xoy$  plane under  $x$ -direction polarization excitation. (a) The electric field distribution of initial states of PIN diodes in the  $x$ -direction. (b) The electric field distribution of adjusting the states of PIN diodes in the  $x$ -direction.

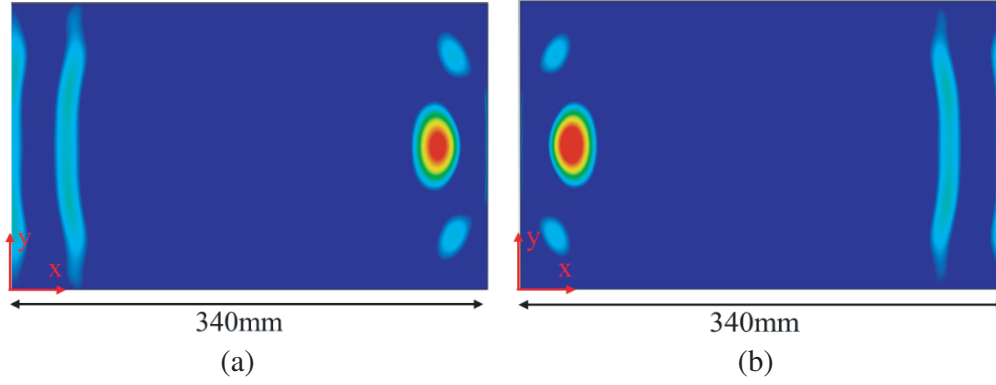
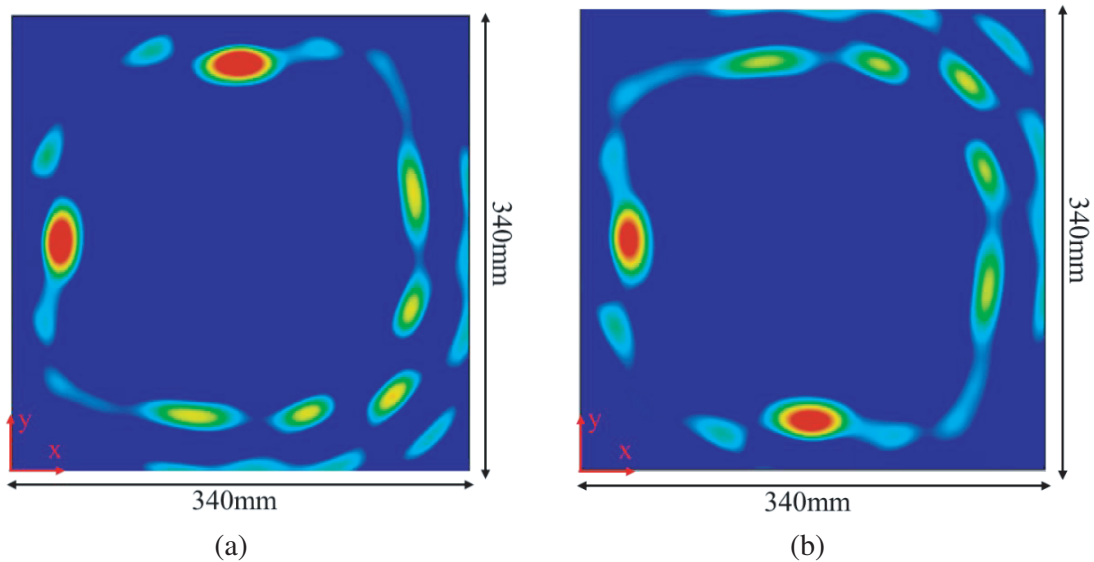


**Figure 11.** Electric field simulation distribution of  $xoy$  plane under  $y$ -direction polarization excitation. (a) The electric field distribution of initial states of PIN diodes in the  $y$ -direction. (b) The electric field distribution of adjusting the states of PIN diodes in the  $y$ -direction.

150 mm, 250 mm). As shown in Fig. 11(b), the position of the maximum electric field intensity in Fig. 11(a) is (141.2 mm, 0, 250 mm), which is basically consistent with the target focus. At the same time, the focus efficiency at 11 GHz is 47.7%. Similarly, adjusting the ON/OFF state of the PIN diodes in the  $y$ -direction on the metasurface, the phase distribution of the metasurface array can be changed. The simulated electric field distribution of  $xoy$  plane is shown in Fig. 11(b). The target focus position is (150 mm, 0, 250 mm), and the position of the maximum electric field intensity in Fig. 11(b) is (140.7 mm, 0, 250 mm), which is basically consistent with the target focus.

To sum up, when the incident wave is a polarized wave in the  $x$ -direction, the focus can be transferred from (0, 140.1 mm, 250 mm) to (0, -140.5 mm, 250 mm) by adjusting the state of the PIN diodes in the  $x$ -direction on the metasurface. When the incident wave is a polarized wave in the  $y$ -direction, the states of the PIN diodes in the  $y$ -direction can also be adjusted to change the focus from (141.2 mm, 0, 250 mm) to (-140.7 mm, 0, 250 mm), achieving the effect of dual polarization dynamic focusing.

Changing the polarization direction of the incident wave, that is, the angle between the electric field vector direction and the  $x$ -axis is  $45^\circ$ . The ratio of the electric field components of  $x$ -polarization and  $y$ -polarization is 1 : 1. The electric field distribution diagram of  $xoy$  plane is shown in Fig. 12(a). By changing the phase arrangement of the focusing metasurface, the simulation results can be obtained in Figs. 12(b), (c), and (d). The Poynting vector integral can be used to calculate the energy ratio of



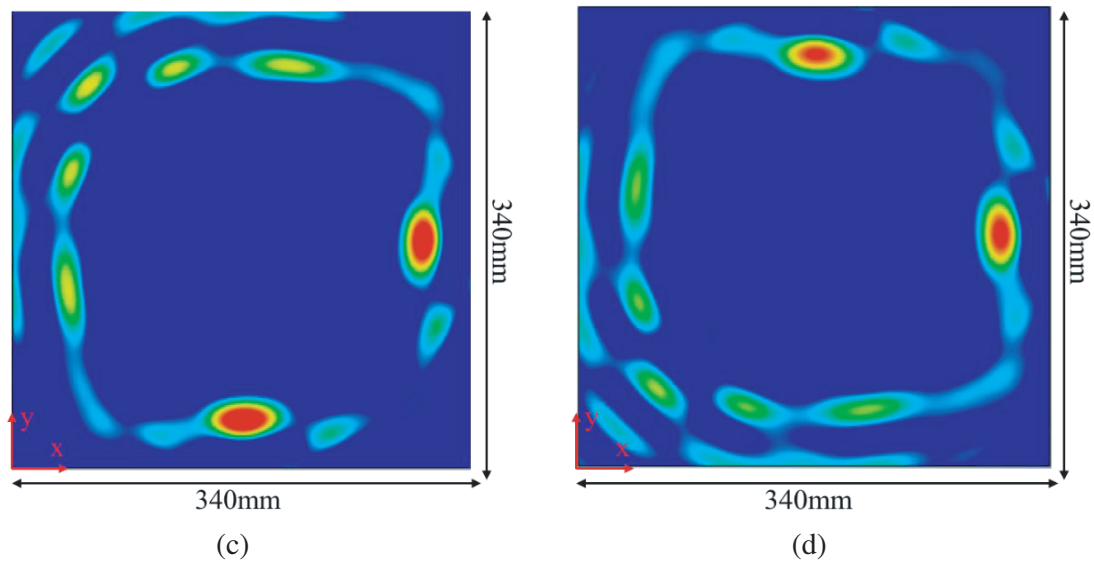


**Figure 12.** Electric field simulation distribution of  $xoy$  plane under  $45^\circ$ -direction polarization excitation. (a) The electric field distribution of initial states of PIN diodes. (b) The electric field distribution of adjusting the states of PIN diodes in the  $x$ -direction. (c) The electric field distribution of adjusting the states of PIN diodes in the  $y$ -direction. (d) The electric field distribution of adjusting the states of PIN diodes in the  $x$ -direction and  $y$ -direction.

the two main focal spots in Fig. 12(a) as 1 : 1, which is in line with the expected result. From the previous Figs. 10 and 11, it can be found that there are some electric field distributions with energy less than the main focal spot in the  $xoy$  plane. When the polarization direction of the incident wave is changed, these electric field distributions are vector superimposed on the horizontal plane to form the auxiliary focal spot on the  $xoy$  plane in Fig. 12. This phenomenon is mainly caused by the accuracy of CST software simulation and the defects of 1-bit reconfigurable metasurface itself.

Similarly, continue to change the polarization direction of the incident wave. The electric field vector and the  $x$ -axis have an angle of  $63.5^\circ$ , that is, the ratio of the electric field components of  $x$ -polarization and  $y$ -polarization is 1 : 2. After the full wave simulation with CST software, the electric field distribution of the  $xoy$  plane can be obtained, as shown in Figs. 13(a) and (b). The Poynting integral of the electric field on the  $xoy$  plane is still carried out, and it can be found that the energy ratio of the two focal spots in Fig. 13(a) is 1 : 2.1, basically in line with the expected result.

Compared with [11] in Table 1, it can be seen that the focusing effect of the unreconfigurable metasurface is better than that of the reconfigurable metasurface, which is also a dual-polarized focusing metasurface. This is because the reconfigurable metasurface can provide an accurate compensation phase, so that the electromagnetic wave can be accurately focused at the expected focus position. However, our work can achieve dynamic focus. Compared with [24] and [22], the 1-bit metasurface unit designed in our work is smaller in size and has larger reflection amplitude at the corresponding frequency point. Therefore, when an array is formed, the overall focusing efficiency is higher. At the

**Table 1.** The comparison of reflective metasurface.

Reference	Working Frequency	Size	Dynamic focusing	Focusing Efficiency
[11]	10 GHz	$13\lambda \times 13\lambda$	No	65.9%
[24]	5.8 GHz	$3.4\lambda \times 3.4\lambda$	Yes	1.5%
[22]	5.8 GHz	$6.5\lambda \times 6.5\lambda$	Yes	30%
our work	11 GHz	$6.9\lambda \times 6.9\lambda$	Yes	47.7%

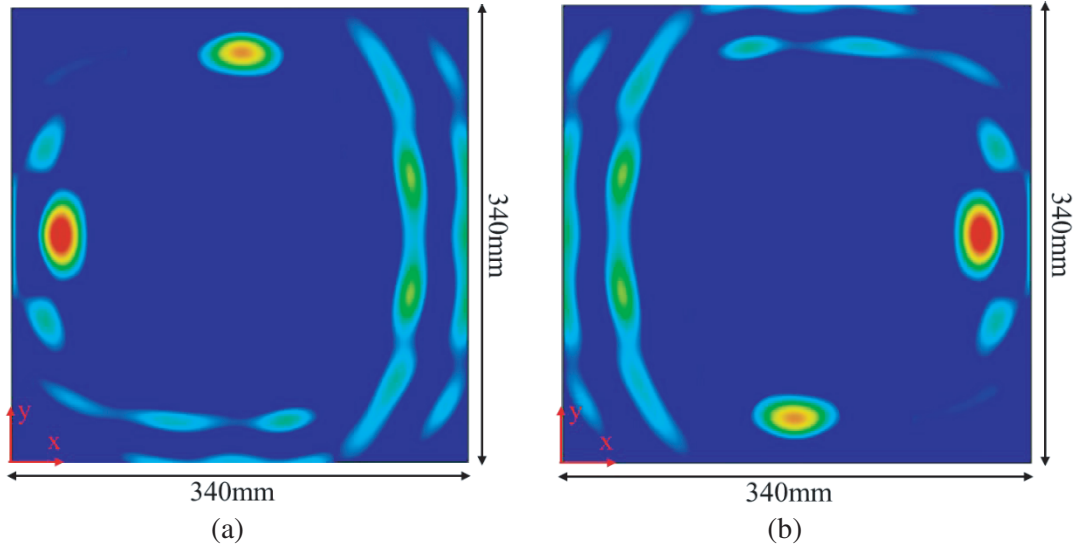


**Figure 13.** Electric field simulation distribution of  $xoy$  plane under  $63.5^\circ$ -direction polarization excitation. (a) The electric field distribution of initial states of PIN diodes in the  $y$ -direction. (b) The electric field distribution of adjusting the states of PIN diodes in the  $x$ -direction.

same time, in our work, by changing the polarization mode of the incident wave and the proportion of the  $x$ -polarization and  $y$ -polarization components, the position transfer of the single focus and the power distribution of the double focus are realized. Realizing dynamic focusing greatly improves the freedom of 1-bit reconfigurable focusing metasurface in the field of wireless power transmission and also improves the utilization of metasurface array.

#### 4. CONCLUSION

In this paper, a 1-bit reconfigurable reflective metasurface unit is proposed, which can achieve dual-polarization focusing effect by using the characteristics of independent control of polarization. The simulation results also verify the effectiveness of the design, changing the polarization direction of the incident wave to regulate the distribution of focus power, and switching the ON/OFF state of the PIN diodes to achieve dynamic focus, which greatly improves the freedom of 1-bit reconfigurable metasurface in the wireless power transmission system, and also shows that 1-bit reconfigurable metasurface has unprecedented potential in the processing of complex electromagnetic waves.

#### ACKNOWLEDGMENT

This work was supported by the Chongqing Graduate Research and Innovation Project (CYS20265).

#### REFERENCES

1. Sri Nagini, K. B. S. and D. S. Chandu, "Wideband and tunable reflective cross-polarization conversion metasurface for terahertz applications," *IEEE Photonics Journal*, Vol. 14, No. 5, 1–8, Oct. 2022.
2. Zhang, B., C. Jin, L. Yin, Q. Lv, P. Zhang, and B. Tian, "Diffusive-Reflective metasurface with dual independent reflection bands for RCS reduction," *IEEE Antennas and Wireless Propagation Letters*, Vol. 21, No. 3, 635–639, Mar. 2022.
3. Jia, Y., G. Jiang, Y. Liu, and Y. Zhong, "Beam scanning for dual-polarized antenna with active reflection metasurface," *IEEE Antennas and Wireless Propagation Letters*, Vol. 21, No. 9, 1722–1726, Sept. 2022.

4. Li, H., G. Li, J. Wang, et al., "Wideband multifunctional metasurface for polarization conversion and gain enhancement," *Progress In Electromagnetics Research*, Vol. 155, 115–125, 2016.
5. Deng, G., Z. Yu, J. Yang, Z. Yin, Y. Li, and B. Chi, "A miniaturized 3-D metamaterial absorber with wide angle stability," *IEEE Microwave and Wireless Components Letters*, Vol. 32, No. 9, 1111–1114, Sept. 2022.
6. Chen, A. and F. Monticone, "Active scattering-cancellation cloaking: Broadband invisibility and stability constraints," *IEEE Transactions on Antennas and Propagation*, Vol. 68, No. 3, 1655–1664, Mar. 2020.
7. Wu, J. L., Y. M. Pan, and S. Y. Zheng, "Design of single-layer polarization-dependent transmissive and reflective focusing metasurface," *IEEE Transactions on Antennas and Propagation*, Vol. 69, No. 11, 7637–7646, Nov. 2021.
8. Sherman, J., "Properties of focused apertures in the fresnel region," *IEEE Transactions on Antennas and Propagation*, Vol. 10, No. 4, 399–408, Jul. 1962.
9. Salah, M., M. M. Elsherbini, and O. A. Omer, "RIS-focus: On the optimal placement of the focal plane for outdoor beam routing," *IEEE Access*, Vol. 10, 53053–53065, 2022.
10. Yu, S., H. Liu, and L. Li, "Design of near-field focused metasurface for high-efficient wireless power transfer with multifocus characteristics," *IEEE Transactions on Industrial Electronics*, Vol. 66, No. 5, 3993–4002, May 2019.
11. Zhang, P., L. Li, X. Zhang, et al., "Design, measurement and analysis of near-field focusing reflective metasurface for dual-polarization and multi-focus wireless power transfer," *IEEE Access*, Vol. 7, 110387–110399, 2019.
12. Wang, D., D. Wang, X. Sun, et al., "Design of a reflective metasurface for near-field focusing," *IEEE International Symposium on Antennas and Propagation and USNC-URSI Radio Science Meeting*, 323–324, 2021.
13. Huang, H. and J. Zhang, "High-efficiency multifunction metasurface based on polarization sensitivity," *IEEE Antennas and Wireless Propagation Letters*, Vol. 20, No. 8, 1508–1512, 2021.
14. Shang, G., H. Li, Z. Wang, et al., "Coding metasurface holography with polarization multiplexed functionality," *Journal of Applied Physics*, Vol. 129, 035304, 2021.
15. Yong, Z., Y. Li and Y. Zhou, "Dynamic manipulation of electromagnetic waves based on 1-bit reconfigurable metasurface," *2022 IEEE 5th International Conference on Electronic Information and Communication Technology*, 519–522, 2022.
16. Yurduseven, O., D. L. Marks, J. N. Gollub, and D. R. Smith, "Design and analysis of a reconfigurable holographic metasurface aperture for dynamic focusing in the fresnel zone," *IEEE Access*, Vol. 5, 15055–15065, 2017.
17. Han, J., L. Li, X. Ma, et al., "Adaptively smart wireless power transfer using 2-bit programmable metasurface," *IEEE Transactions on Industrial Electronics*, Vol. 69, No. 8, 8524–8534, 2022.
18. Gao, X., W. L. Yang, H. F. Ma, Q. Cheng, X. H. Yu, and T. J. Cui, "A reconfigurable broadband polarization converter based on an active metasurface," *IEEE Transactions on Antennas and Propagation*, Vol. 66, No. 11, 6086–6095, Nov. 2018.
19. Ma, Q., W. Gao, Q. Xiao, et al., "Directly wireless communication of human minds via non-invasive brain-computer-metasurface platform," *eLight*, Vol. 2, No. 1, 11, 2022.
20. Li, L., H. Zhao, C. Liu, et al., "Intelligent metasurfaces: Control, communication and computing," *eLight*, Vol. 2, 7, 2022.
21. Ratni, B., Z. Wang, K. Zhang, et al., "Reconfigurable reflective metasurface for dynamic control of focal point position," *2019 13th European Conference on Antennas and Propagation*, 1–3, 2019.
22. Yu, W. and H. Lin, "Application of 2-bit reconfigurable reflectarray in near-field wireless power transmission," *2021 International Conference on Microwave and Millimeter Wave Technology*, 1–3, 2021.
23. Kraus, J. D., *Antenna*, Publishing House of Electronics Industry, 2015.
24. Tran, N. M., M. M. Amri, J. H. Par, et al., "A novel coding metasurface for wireless power transfer applications," *Energies*, Vol. 12, 4488, 2019.